Approximating Decoding Thresholds of Punctured LDPC Code Ensembles on the AWGN Channel

Mitchell, David G.M.; Lentmaier, Michael; Pusane, Ali E.; Costello Jr., Daniel J.

Published in:
2015 IEEE International Symposium on Information Theory (ISIT)

DOI:
10.1109/ISIT.2015.7282489

2015

Approximating Decoding Thresholds of Punctured LDPC Code Ensembles on the AWGN Channel

David G. M. Mitchell*, Michael Lentmaier†, Ali E. Pusane‡, and Daniel J. Costello, Jr.*
*Dept. of Electrical Engineering, University of Notre Dame, Notre Dame, Indiana, USA, {david.mitchell, costello.2}@nd.edu
†Dept. of Electrical and Information Technology, Lund University, Lund, Sweden, Michael.Lentmaier@eit.lth.se
‡Dept. of Electrical and Electronics Engineering, Bogazici University, Istanbul, Turkey, ali.pusane@boun.edu.tr

***Abstract*—In this paper, we provide an efficient way to predict iterative belief propagation (BP) decoding thresholds of randomly punctured low-density parity-check (LDPC) code ensembles on the binary-input additive white Gaussian noise channel (AWGNC), given only the BP threshold of the mother code ensemble on the binary erasure channel (BEC) and the code design rate. We show that the predictions are accurate by comparing them with values calculated by discretized density evolution for a variety of puncturing fractions. We find that the strength and suitability of an LDPC code ensemble for random puncturing over the AWGNC with respect to iterative decoding threshold is completely determined by a single constant θ, and this behavior is demonstrated using both LDPC block code and spatially coupled LDPC code ensembles. Finally, we present simulation results that confirm the excellent decoding performance promised by the asymptotic results.**

I. Introduction

It is often desirable in applications that experience changing channel conditions to be able to employ a variety of code rates. One method to achieve this is to *puncture* a low rate mother code. In this scheme, the transmitter punctures coded symbols, and, as a result of having fewer transmitted code symbols, the code rate is increased. It is assumed that the receiver knows the positions of the punctured symbols, so that both the punctured and transmitted symbols can be estimated during decoding. Coding schemes that use this technique are known as *rate-compatible punctured codes* [1]. Since the decoder for the mother code is used to decode the punctured codes, a variety of code rates can be achieved using the same decoding architecture by puncturing different numbers of symbols. Punctured low-density parity-check (LDPC) codes have been extensively studied in the literature (see, *e.g.*, [2], [3], [4], [5]).

It was shown in [6] that, over the binary erasure channel (BEC), transmission of a randomly punctured code ensemble can be modeled as two cascaded BECs or, equivalently, a single BEC with a modified erasure rate. Consequently, it was shown that, with respect to the iterative belief propagation (BP) decoding threshold, the strength and suitability of an LDPC code ensemble for random puncturing over the BEC is completely determined by a single constant $\theta \geq 1$ that depends only on the rate and the BP threshold of the mother code ensemble. If $\theta = 1$, the punctured ensembles are capacity achieving for all higher rates, and if θ is close to 1, the punctured ensemble thresholds are close to capacity for all higher rates up to $1/\theta$.

In this paper, we extend the results of [6] to the binary-input additive white Gaussian noise channel (AWGNC) and show that analogous results can be obtained. In particular, we develop a relationship between the BP thresholds on the two channels and provide an efficient way to predict the thresholds of punctured LDPC code ensembles on the AWGNC given only the BP threshold of the mother code ensemble on the BEC and the code design rate. The predictions are shown to be accurate by comparing them with values calculated by discretized density evolution for a variety of code ensembles and puncturing fractions. Both LDPC block code (LDPC-BC) and spatially coupled LDPC (SC-LDPC) code ensembles are used to demonstrate the behavior. Finally, computer simulations are presented that confirm the robust decoding performance promised by the asymptotic results.

II. Randomly Punctured LDPC Codes

In this section, we begin by describing protograph based LDPC-BCs and SC-LDPC codes. We continue by describing the process of randomly puncturing LDPC codes and provide a brief summary of previous results obtained for the BEC.

A. Protograph-based LDPC-BCs

A protograph [7] with *design rate* $R = 1 - n_c/n_v$ is a small bipartite graph that connects a set of n_v variable nodes to a set of n_c check nodes by a set of edges. The protograph can be represented by a parity-check or *base* biadjacency matrix $\mathbf{B}$, where $B_{x,y}$ is taken to be the number of edges connecting variable node v_y to check node c_x. The parity-check matrix $\mathbf{H}$ of a protograph-based LDPC-BC can be created by replacing each non-zero entry in $\mathbf{B}$ by a sum of $B_{x,y}$ non-overlapping permutation matrices of size $M \times M$ and each zero entry by the $M \times M$ all-zero matrix. It is an important feature of this construction that each derived code inherits the degree distribution and graph neighborhood structure of the protograph. The ensemble of protograph-based LDPC-BCs with block length $n = Mn_v$ is defined by the set of matrices $\mathbf{H}$ that can be derived from a given protograph using all possible combinations of $M \times M$ permutation matrices. We denote the (J, K)-regular LDPC-BC ensemble defined by the all-ones base matrix $\mathbf{B}$ of size $J \times K$ as $\mathcal{B}_{J,K}$.

B. Protograph-based SC-LDPC Codes

SC-LDPC codes are constructed by *coupling* together a series of L disjoint, or uncoupled, Tanner graphs of an LDPC-BC into a single coupled chain. SC-LDPC codes have been shown to combine excellent iterative decoding thresholds [8], [9] and good asymptotic minimum distance properties [10]. Moreover, it has been proven analytically for general

Ensemble	Component base matrices
$\mathcal{C}_{3,4}(L)$	$\mathbf{B}_0 = \begin{bmatrix} 1 & 1 & 0 & 0 \\ 0 & 1 & 1 & 0 \\ 0 & 0 & 1 & 1 \end{bmatrix}, \mathbf{B}_1 = \begin{bmatrix} 0 & 0 & 1 & 1 \\ 1 & 0 & 0 & 1 \\ 1 & 1 & 0 & 0 \end{bmatrix}$
$\mathcal{C}_{3,6}(L)$	$\mathbf{B}_0 = \mathbf{B}_1 = \mathbf{B}_2 = [\ 1 \quad 1\ ]$
$\mathcal{C}_{3,6,B}(L)$	$\mathbf{B}_0 = [\ 1 \quad 1\ ], \mathbf{B}_1 = [\ 2 \quad 2\ ]$

TABLE I: SC-LDPC code ensemble component base matrices.

memoryless binary-input symmetric-output (MBS) channels that the BP decoding thresholds of a class of (J, K)-regular SC-LDPC code ensembles achieve the maximum a posteriori probability (MAP) decoding thresholds of the underlying (J, K)-regular LDPC-BC ensembles, a phenomenon termed *threshold saturation* [9].

Starting from a $b_c \times b_v$ block base matrix $\mathbf{B}$, an "edge-spreading" construction [10] can be used to form the base matrix of an SC-LDPC code ensemble with *coupling length* L as

$$\mathbf{B}_{[0,L-1]} = \begin{bmatrix} \mathbf{B}_0 & & & \\ \mathbf{B}_1 & \mathbf{B}_0 & & \\ \vdots & \mathbf{B}_1 & \ddots & \\ \mathbf{B}_w & \vdots & \ddots & \mathbf{B}_0 \\ & \mathbf{B}_w & & \mathbf{B}_1 \\ & & \ddots & \vdots \\ & & & \mathbf{B}_w \end{bmatrix}_{(L+w)b_c \times Lb_v}, \quad (1)$$

where $\mathbf{B}_0 + \mathbf{B}_1 + \cdots \mathbf{B}_w = \mathbf{B}$, w denotes the *coupling width*, and the $b_c \times b_v$ *component base matrices* $\mathbf{B}_i$, $i = 0, 1, \ldots, w$, represent the edge connections from the b_v variable nodes at time t to the b_c check nodes at time $t + i$. An ensemble of SC-LDPC codes can then be formed from $\mathbf{B}_{[0,L-1]}$ using the protograph construction method described above. The design rate of the ensemble of SC-LDPC codes is

$$R_L = 1 - \frac{(L+w)b_c}{Lb_v}, \quad (2)$$

where we note that R_L is monotonically increasing and approaches $1 - b_c/b_v$ as $L \to \infty$. The ensembles and their component base matrices that we use in this paper are given in Table I.

C. Puncturing Linear Codes

A linear code is *punctured* by removing a set of p columns from its generator matrix, which has the effect of reducing the codeword length from n to $n - p$. After puncturing a linear code with *puncturing fraction* $\alpha = p/n$, the resulting transmission rate is

$$R(\alpha) = \frac{R}{1-\alpha}, \quad \alpha \in [0, 1), \quad (3)$$

where $R(0) = R$ is the rate of the mother (unpunctured) code. A code can be punctured randomly or according to a particular pattern. It is assumed that the receiver knows the positions of the punctured bits, and the decoder estimates both the punctured and transmitted symbols during decoding.

D. BEC Thresholds of Punctured LDPC Code Ensembles

In [6], it was shown that the channel model for random puncturing of an LDPC code on the BEC can be considered as two cascaded BECs or, equivalently, a single BEC with a modified erasure rate. Consequently, it was shown that the BEC threshold $\epsilon_{\text{BP}}(\alpha)$ of a randomly punctured code ensemble with puncturing fraction α is

$$\epsilon_{\text{BP}}(\alpha) = 1 - \frac{1 - \epsilon_{\text{BP}}(0)}{R} \cdot R(\alpha). \quad (4)$$

Remarkably, $\epsilon_{\text{BP}}(\alpha)$ is simply a function of the target rate $R(\alpha) \geq R$, i.e., for a given puncturing fraction α, the function $\epsilon_{\text{BP}}(\alpha)$ depends only on the threshold and the rate of the mother code ensemble. From (4), we define

$$\theta = \frac{1 - \epsilon_{\text{BP}}(0)}{R} \geq 1, \quad (5)$$

where equality holds if and only if the threshold of the mother code ensemble is equal to the Shannon limit which, in turn, implies that the Shannon limit can be achieved for all rates $R(\alpha) \geq R$.

The strength and suitability of an LDPC code ensemble for random puncturing is characterized completely by θ. For example, the $(3, 6)$-regular ensemble $\mathcal{B}_{3,6}$ is better suited for random puncturing than the $(4, 8)$-regular ensemble $\mathcal{B}_{4,8}$, since the respective values of θ are 1.1411 and 1.2331, respectively. Values of θ for a variety of LDPC and SC-LDPC code ensembles can found in [6]. Finally, we note that the largest possible rate obtainable by puncturing a particular ensemble is determined by the smallest non-negative threshold $\epsilon_{\text{BP}}(\alpha)$, which yields

$$R_{\max} = R(\alpha = \epsilon_{\text{BP}}(0)) = \frac{1}{\theta}. \quad (6)$$

It follows that the maximum puncturing fraction α with non-vanishing BP threshold is equal to the BEC threshold $\epsilon_{\text{BP}}(0) = \epsilon_{\text{BP}}$ of the mother code ensemble.

III. Thresholds of Punctured LDPC Code Ensembles on the AWGNC

In this section, we investigate the BP thresholds of randomly punctured LDPC code ensembles on the AWGNC. We begin by calculating some numerical results for a variety of ensembles and puncturing fractions. We then provide an efficient way to accurately predict the BP thresholds of randomly punctured LDPC code ensembles on the AWGNC, given only the BP threshold of the mother code ensemble on the BEC. Finally, we briefly discuss the implications of these results.

A. Numerical Results

In Fig. 1, we display calculated AWGNC BP thresholds of the randomly punctured LDPC-BC ensembles $\mathcal{B}_{3,6}^{\text{punc}}(\alpha)$ and SC-LDPC code ensembles $\mathcal{C}_{3,6}^{\text{punc}}(L, \alpha)$ for $L = 10, 20, 100$ and a variety of puncturing fractions α. The thresholds were obtained using discretized density evolution for the AWGNC and are shown in terms of noise standard deviation σ (left) and E_b/N_0 (right). We observe that random puncturing of LDPC-BC and SC-LDPC code ensembles displays robust threshold performance, in the sense that, as we increase the puncturing fraction α, the thresholds do not significantly degrade and roughly track the capacity curve. To be more precise, we observe that, if the mother code ensemble has a threshold close to capacity (e.g., the $\mathcal{C}_{3,6}^{\text{punc}}(100, 0)$ ensemble), then as α is increased the gap to capacity increases slowly and the calculated thresholds track the capacity curve closely. On the

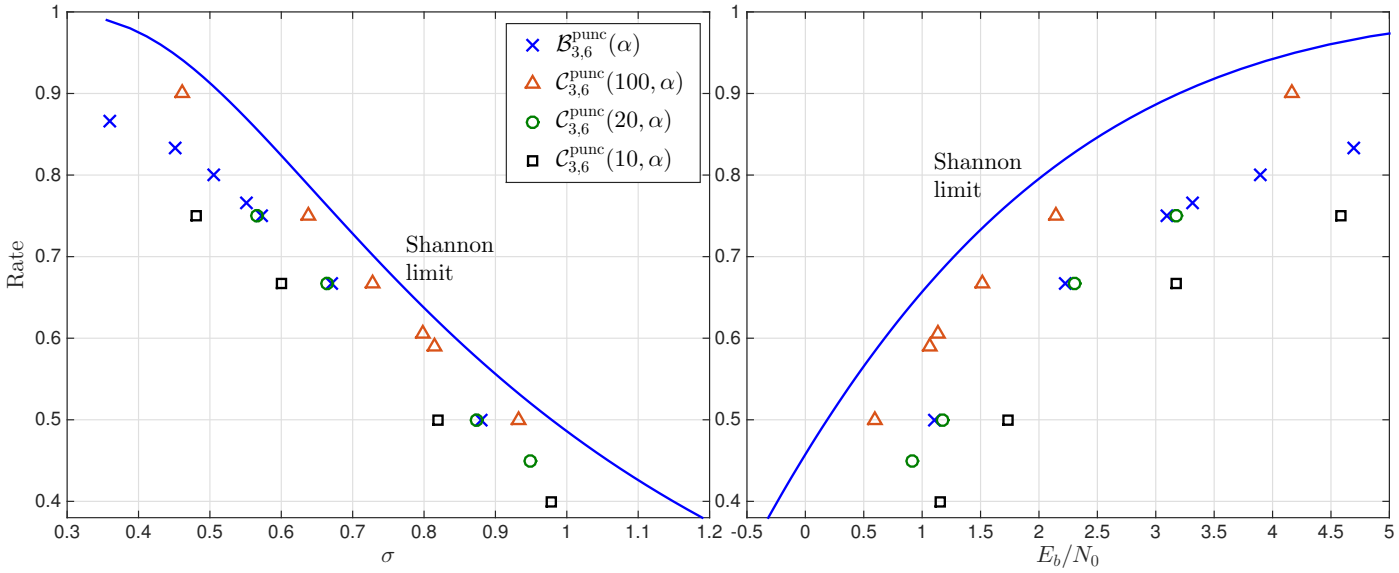

Fig. 1: Numerically calculated AWGNC BP thresholds of several randomly punctured LDPC-BC and SC-LDPC code ensembles for a variety of puncturing fractions. Thresholds are shown in terms of noise standard deviation σ (left) and E_b/N_0 (right).

other hand, if the mother code ensemble has a threshold further from capacity (e.g., the $\mathcal{C}_{3,6}^{\text{punc}}(10,0)$ ensemble), then the gap to capacity increases faster with increasing α.

The analogous analytical result for the BEC follows directly from (4), where it can be seen that the gap to capacity of any punctured ensemble is determined by the constant θ from (5), where the thresholds of the punctured ensembles lie on a straight line for which the slope is determined by θ (see [6] for further details). Finally, as α increases, we find that the maximum achievable rate, i.e., the maximum $R(\alpha)$ where an AWGNC BP threshold exists, is approximately equal to the value computed for the BEC using (6).

B. Predicting Thresholds

Given the similarities between the threshold results for the BEC and AWGNC, a natural question arises: is it possible to predict the behavior of the thresholds of randomly punctured code ensembles on the AWGNC in a similar way as for the BEC? Recall that the capacity of a BEC with erasure probability ϵ is $C_{\text{BEC}}(\epsilon) = 1-\epsilon$, so that (4) can be written as

$$\epsilon_{\text{BP}}(\alpha) = 1 - \theta \cdot R(\alpha) = C_{\text{BEC}}^{-1}(\theta \cdot R(\alpha)) = C_{\text{BEC}}^{-1}(f(R(\alpha))),$$

which converges to zero as $f(R(\alpha)) = \theta \cdot R(\alpha) \to 1$. The thresholds shown in Fig. 1 suggest the existence of a similar relationship for the AWGNC, i.e.,

$$\sigma_{\text{BP}}(\alpha) = C_{\text{AWGNC}}^{-1}(f(R(\alpha))) \tag{7}$$

for some function $f(R(\alpha))$, where $C_{\text{AWGNC}}(\sigma)$ denotes the capacity of the AWGNC and $\sigma_{\text{BP}}(\alpha)$ is the BP threshold in terms of the noise standard deviation σ.[1] Note that $\sigma_{\text{Sh}} = C_{\text{AWGNC}}^{-1}(R(\alpha))$ denotes the Shannon limit for a given rate $R(\alpha)$, which implies that the function $f(R(\alpha))$ characterizes the gap between the BP threshold and the Shannon limit for all achievable rates $R(\alpha) \geq R$.

[1]Note that $C_{\text{BEC}}(x) = C_{\text{BEC}}^{-1}(x)$, but $C_{\text{AWGNC}}(x) \neq C_{\text{AWGNC}}^{-1}(x)$.

In order to identify the shape of $f(R(\alpha))$, we consider the AWGNC entropy of the BP thresholds, i.e., $h(\sigma_{\text{BP}}(\alpha)) = 1 - C_{\text{AWGNC}}(\sigma_{\text{BP}}(\alpha))$.[2] In Fig. 2, the thresholds (crosses, triangles, circles, and squares) $h(\sigma_{\text{BP}}(\alpha))$ are plotted against the rate $R(\alpha)$, along with the capacity $C_{\text{AWGNC}}(\sigma) = 1-h(\sigma)$. Interestingly, we find that, as for the BEC channel, a linear relationship appears to exist between $h(\sigma_{\text{BP}}(\alpha))$ and $R(\alpha)$. To approximate the slope, one can obtain a θ_{AWGNC} similar to θ_{BEC}, but based on the AWGNC BP threshold $h(\sigma_{\text{BP}}(0))$ and design rate $R = R(0)$ of the mother code ensemble as

$$\theta_{\text{AWGNC}} = \frac{1 - h(\sigma_{\text{BP}}(0))}{R} \geq 1. \tag{8}$$

Numerically, we find that $\theta_{\text{AWGNC}} \approx \theta_{\text{BEC}}$ for all of the code ensembles considered; consequently, we use θ_{BEC} to obtain predicted AWGNC thresholds in the remainder of the paper. Using $f(R(\alpha)) = \theta_{\text{BEC}} \cdot R(\alpha)$, we obtain the expression

$$h(\sigma_{\text{BP}}(\alpha)) \approx 1 - \theta_{\text{BEC}} \cdot R(\alpha), \tag{9}$$

where θ_{BEC} is calculated using (5). Predicted AWGNC threshold values using (9) are included in Fig. 2 as solid lines. We observe that, remarkably, the approximations are very good even though the value is immediately obtained for any target rate using only θ_{BEC}, which depends on the BEC threshold and rate of the mother code ensemble.[3] Finally, we note from (9) that thresholds cease to exist at precisely the same R_{max} as calculated for the BEC using (6).

Assuming $f(R(\alpha)) = \theta_{\text{BEC}} \cdot R(\alpha)$, we can predict thresholds in terms of noise standard deviation as

$$\sigma_{\text{BP}}(\alpha) \approx C_{\text{AWGNC}}^{-1}(\theta_{\text{BEC}} \cdot R(\alpha)). \tag{10}$$

[2]For the BEC we have $h_{\text{BEC}}(\epsilon) = 1 - C_{\text{BEC}}(\epsilon) = \epsilon$.

[3]We observe a slight difference in the calculated threshold when compared to the prediction in some cases, particularly for small α, as can be seen in Fig. 2. This difference could be a weakness in the prediction method and/or simply a result of the numerical inaccuracy of performing discretized density evolution on the AWGNC.

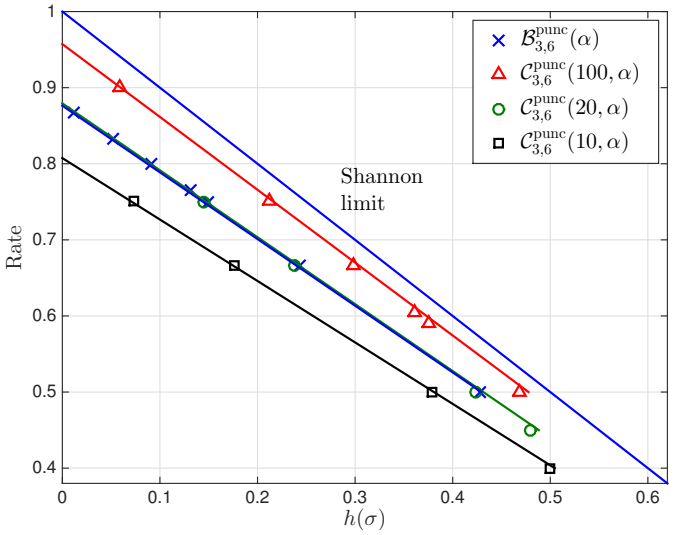

Fig. 2: Numerically calculated AWGNC BP thresholds in terms of the entropy $h(\sigma_{\text{BP}}(\alpha))$ of several randomly punctured LDPC-BC and SC-LDPC code ensembles (crosses, triangles, circles, and squares) for a variety of puncturing fractions. Also shown are the predicted thresholds (solid lines).

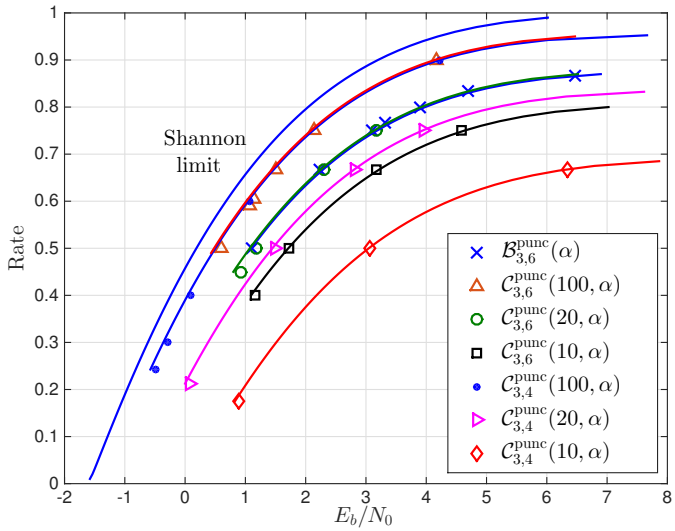

Fig. 3: Numerically calculated AWGNC BP thresholds in terms of E_b/N_0 of several randomly punctured LDPC-BC and SC-LDPC code ensembles (crosses, triangles, circles, and squares) for a variety of puncturing fractions. Also shown are the predicted thresholds (solid lines).

Fig. 3 displays some calculated AWGNC BP thresholds in terms of E_b/N_0 of several randomly punctured LDPC-BC and SC-LDPC code ensembles (crosses, triangles, circles, and squares) for a variety of puncturing fractions along with the predicted thresholds for rates up to $R_{\text{max}} = 1/\theta_{\text{BEC}}$. Again, we observe that the predictions are a good fit with the calculated values obtained using discretized density evolution, and that the mother code ensembles with thresholds closer to capacity have curves that closely track the capacity curve.

C. Discussion

There are several important implications of the results presented above.

- Equation (10) permits a quick and easy way to approximate AWGNC thresholds for any LDPC code ensemble, punctured or unpunctured, given only the BEC BP threshold and design rate. For example, the $(3,6)$-regular ensemble $\mathcal{B}_{3,6}$ has $\theta_{\text{BEC}} = 1.1411$ and a quick calculation using (10) gives $\sigma_{\text{BP}} = 0.881$, which agrees exactly with the known value [11]. This approximation implies that we assume the AWGNC entropy evaluated at the threshold is close to the entropy of the BEC in both the punctured and unpunctured cases, i.e., $h(\sigma_{\text{BP}}(\alpha)) \approx h_{\text{BEC}}(\epsilon_{\text{BP}}(\alpha))$ for all $\alpha \geq 0$. Future work will involve an investigation of the accuracy of the prediction for general LDPC-BC and SC-LDPC code ensembles.
- By extension, and using the analysis presented in [6] for the BEC, thresholds can easily be obtained for any randomly punctured LDPC code ensemble on the BEC and AWGNC. We saw for both channel models that the thresholds of randomly punctured code ensembles depend solely on θ_{BEC}: a large value of θ_{BEC} implies that the mother code ensemble has a threshold relatively far from the Shannon limit and the gap to capacity grows quickly with increasing α; on the other hand, for a value of θ_{BEC} close to 1, the mother code ensemble has a threshold close to the Shannon limit and the gap to capacity grows slowly with increasing α.
- Ensembles with similar values of θ_{BEC} will perform roughly as well for all achievable rates, even if their design rates are different. For example, we calculate the θ_{BEC} values for the $\mathcal{C}_{3,4}(100)$ and $\mathcal{C}_{3,6}(100)$ ensembles as 1.044 and 1.048, respectively. Consequently, their thresholds, as observed in Fig. 3, are approximately equal for all higher achievable rates. Note that this demonstrates that if one punctures a lower rate ensemble with a larger puncturing fraction than a higher rate ensemble in order to achieve a desired rate, there is no penalty in threshold as long as the values of θ_{BEC} are similar.
- If one can find a capacity approaching or capacity achieving code ensemble then it will have a θ_{BEC} value close to, or equal to, 1 and it will be well suited to random puncturing. Related statements regarding capacity achieving LDPC code ensembles on the BEC with puncturing have been made before (see *e.g.*, [4], [12]). We have chosen to use SC-LDPC code ensembles in this paper to demonstrate the effects of random puncturing since SC-LDPC code ensembles possess a combination of good θ_{BEC} values and linear minimum distance growth (see [6]). Without spatial coupling, one would have to design an optimized (irregular) LDPC-BC ensemble to obtain a good value of θ_{BEC}, or accept a poor value of θ_{BEC} with a (J,K)-regular LDPC-BC ensemble. However, designing optimized irregular mother LDPC-BC code ensembles to obtain a good value of θ_{BEC} is likely to result in poor minimum distance properties.

IV. Finite Length Performance of Randomly Punctured LDPC Code Ensembles

The bit error rate (BER) performance of randomly punctured SC-LDPC codes transmitted over the AWGNC was also investigated via computer simulations. A mother code with code length $n = 50,000$ was drawn from the ensemble $\mathcal{C}_{3,6,B}(L = 50)$ with protograph lifting factor $M = 500$. This

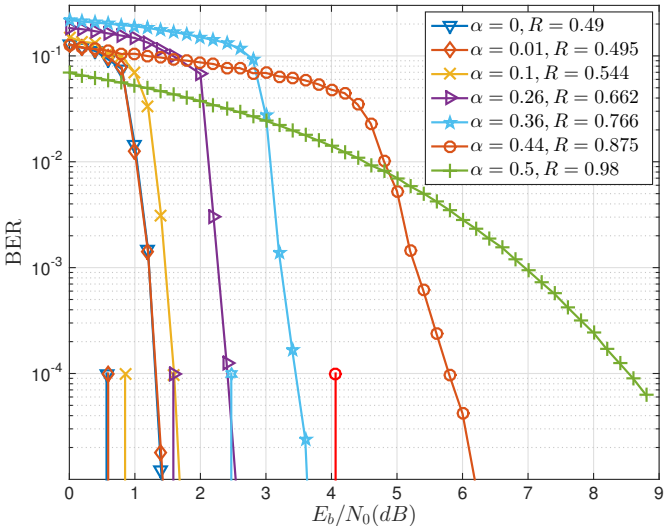

Fig. 4: AWGNC decoding error performance of randomly punctured SC-LDPC codes drawn from $\mathcal{C}^{\text{punc}}_{3,6,B}(50,\alpha)$ with protograph lifting factor $M = 500$. Also shown for comparison are the predicted BP thresholds for the punctured SC-LDPC code ensembles $\mathcal{C}^{\text{punc}}_{3,6,B}(50,\alpha)$.

code has a rate of $R_{50} = 0.49$. The code rate was increased by randomly puncturing the code with puncturing fractions $\alpha = 0.01, 0.1, 0.26, 0.36, 0.44$, and 0.5, yielding code rates of $R(0.01) = 0.495$, $R(0.1) = 0.544$, $R(0.26) = 0.662$, $R(0.36) = 0.766$, $R(0.44) = 0.875$, and $R(0.5) = 0.98$, respectively. The error performance of these codes was obtained using a sliding window decoder (WD) [8] with window size $W = 8$ (corresponding to $2WM = 8000$ bits) and performing a maximum of $I = 100$ iterations in each window position. The results for these codes are presented in Fig. 4 along with the predicted thresholds obtained using (7), where we calculated a WD threshold of $\epsilon_{\text{BP}} = 0.4777$, and consequently $\theta_{\text{BEC}} = 1.0659$.

We observe robust decoding performance from the punctured SC-LDPC codes of varying rates.[4] We note that it appears that the gap between the simulated decoding performance and the corresponding predicted threshold increases slightly as the puncturing fraction α increases. For example, when α is moderate, e.g., $\alpha = [0, 0.36]$, each code displays a gap from its respective predicted iterative decoding threshold of approximately 0.8 to 1dB at a BER of 10^{-5}, whereas for $\alpha = 0.44$ the gap increases to about 2dB. This should be expected for a finite length protograph-based code with small lifting factor M; however, we expect these gaps to decrease as M increases.

Since the capacity and threshold prediction curves are not linear (see, e.g., Fig. 3), the closer we get to the maximum rate R_{max}, the more significant the gap to capacity, i.e., we observe that the slope of the threshold curve flattens out (tracking the capacity curve) for higher rate punctured ensembles. It follows that, as the target rate increases past a certain point, the thresholds significantly degrade and the corresponding simulated performance moves further to the right. Moreover, as the puncturing fraction becomes too large (in this case $R(\alpha) > R_{\text{max}} = 1/\theta_{\text{BEC}} = 0.938$), the threshold no longer exists and we do not observe the waterfall performance normally associated with codes operating below their threshold. Recall that ensembles with poor θ_{BEC} values are characterized by a smaller maximum rate R_{max}. For example, the $\mathcal{B}_{3,6}$ ensemble can only be punctured up to $R_{\text{max}} = 0.876$.

[4]Simulation results for randomly punctured $\mathcal{C}^{\text{punc}}_{3,6,B}(50,\alpha)$ ensembles on the BEC were obtained in [6], where similarly robust performance was observed.

V. Concluding Remarks

In this paper, we have provided an efficient way to predict BP thresholds of punctured LDPC code ensembles on the binary-input AWGNC, given only the BP threshold of the mother code ensemble on the BEC and the design rate. We showed that the predictions were accurate by comparing them with values calculated using discretized density evolution for a variety of puncturing fractions. We found that, analogous to the BEC, the strength and suitability of an LDPC code ensemble for random puncturing over the AWGNC with respect to iterative decoding threshold is completely determined by a single constant θ. The approach was demonstrated for both LDPC-BC and SC-LDPC code ensembles and simulation results were provided to confirm the excellent decoding performance promised by the asymptotic results.

Acknowledgment

This work was partially supported by NSF Grant CCF-1161754 and TUBITAK Grant 111E276.

References

[1] J. Hagenauer, "Rate-compatible punctured convolutional codes (RCPC codes) and their applications," *IEEE Trans. Communications*, vol. 36, no. 4, pp. 389–400, Apr. 1988.

[2] J. Ha, J. Kim, and S. W. McLaughlin, "Rate-compatible puncturing of low-density parity-check codes," *IEEE Trans. Inf. Theory*, vol. 50, no. 11, pp. 2824–2836, Nov. 2004.

[3] J. Ha, J. Kim, D. Klinc, and S. W. McLaughlin, "Rate-compatible punctured low-density parity-check codes with short block lengths," *IEEE Trans. Inf. Theory*, vol. 52, no. 2, pp. 728–738, Feb. 2006.

[4] H. Pishro-Nik and F. Fekri, "Results on punctured low-density parity-check codes and improved iterative decoding techniques," *IEEE Transactions on Inf. Theory*, vol. 53, no. 2, pp. 599–614, Feb. 2007.

[5] T. Van Nguyen, A. Nosratinia, and D. Divsalar, "The design of rate-compatible protograph LDPC codes," *IEEE Trans. Communications*, vol. 60, no. 10, pp. 2841–2850, Oct. 2012.

[6] D. G. M. Mitchell, M. Lentmaier, A. E. Pusane, and D. J. Costello, Jr., "Randomly punctured spatially coupled LDPC codes," in *Proc. Int. Symp. Turbo Codes and Iterative Inf. Processing*, Bremen, Germany, Aug. 2014, pp. 1–6.

[7] J. Thorpe, "Low-density parity-check (LDPC) codes constructed from protographs," Jet Propulsion Laboratory, Pasadena, CA, INP Progress Report 42-154, Aug. 2003.

[8] M. Lentmaier, A. Sridharan, D. J. Costello, Jr., and K. Sh. Zigangirov, "Iterative decoding threshold analysis for LDPC convolutional codes," *IEEE Trans. Inf. Theory*, vol. 56, no. 10, pp. 5274–5289, Oct. 2010.

[9] S. Kudekar, T. Richardson, and R. Urbanke, "Spatially coupled ensembles universally achieve capacity under belief propagation," *IEEE Trans. Inf. Theory*, vol. 59, no. 12, pp. 7761–7813, Dec. 2013.

[10] D. G. M. Mitchell, M. Lentmaier, and D. J. Costello, Jr., "Spatially coupled LDPC codes constructed from protographs," *submitted to the IEEE Trans. Inf. Theory*, 2014. [Online]. Available: http://arxiv.org/abs/1407.5366

[11] T. J. Richardson and R. L. Urbanke, *Modern coding theory*. Cambridge University Press, 2008.

[12] C.-H. Hsu and A. Anastasopoulos, "Capacity-achieving codes with bounded graphical complexity and maximum likelihood decoding," *IEEE Trans. Inf. Theory*, vol. 56, no. 3, pp. 992–1006, Mar. 2010.